

Diversity in the Persistence of El Niño Events Over the Last Millennium

Sara C. Sanchez¹  and Kristopher B. Karnauskas^{1,2} ¹Department of Atmospheric and Oceanic Sciences, University of Colorado Boulder, Boulder, CO, USA, ²Cooperative Institute for Research in Environmental Sciences (CIRES), University of Colorado Boulder, Boulder, CO, USA**Key Points:**

- We find consistent evidence of multi-year El Niño events in instrumental observations, paleoclimate archives, and global climate models
- The characteristics of these events vary at low frequencies. At centennial timescales, such variation is indistinguishable from random noise
- Multi-year El Niños are often among the largest events, with implications for global precipitation and temperature impacts

Supporting Information:

Supporting Information may be found in the online version of this article.

Correspondence to:S. C. Sanchez,
sara.sanchez@colorado.edu**Citation:**Sanchez, S. C., & Karnauskas, K. B. (2021). Diversity in the persistence of El Niño events over the last millennium. *Geophysical Research Letters*, 48, e2021GL093698. <https://doi.org/10.1029/2021GL093698>

Received 8 APR 2021

Accepted 2 SEP 2021

Abstract The El Niño Southern Oscillation (ENSO) is a mode of internal climate variability with far-reaching impacts. Here, we consider an important aspect of ENSO behavior: the diversity in the persistence of El Niño events. We examine the occurrence of multi-year El Niño events in instrumental observations, a suite of global climate model simulations of the last millennium, and paleoclimate archives. We find evidence of multi-year El Niño events in all data sources considered, with a wide range of variability in the frequency of such events across and within the individual sources. Although scarce over the relatively brief satellite era, multi-year El Niño events are often associated with the warmest El Niño events in observations and most models. Furthermore, we show that multi-year El Niño events augment the persistence of associated hydroclimate anomalies, which may compound the impacts on vulnerable economies and ecosystems within and beyond the tropical Pacific sector.

Plain Language Summary A typical El Niño event spans a single year, but on occasion, an El Niño event can span multiple, consecutive years. Here we investigate unusually persistent El Niño events in instrumental observations, 11 different climate models that simulate the climate of the last millennium, and in temperature sensitive paleoarchives from the central equatorial Pacific. Multi-year El Niño events are found in observations, all models, and paleoarchives over the course of the last millennium, albeit with much diversity between the various simulations and observations. In an individual product or simulation, there are oftentimes centuries with many multi-year El Niño events followed by centuries with few multi-year events. Many of the largest El Niño events found in observations, climate model simulations, and paleoarchives feature this unusual persistence. Additionally, these multi-year events can cause persistent impacts in global precipitation and surface temperatures.

1. Introduction

The El Niño-Southern Oscillation (ENSO) is the dominant mode of interannual variability on the planet, involving powerful feedbacks between the tropical Pacific Ocean and overlying atmospheric (Walker) circulation (Bjerknes, 1969). The ENSO system oscillates between two phases, a warm El Niño state and a cool La Niña state; both are capable of exerting considerable influence on global anomalies of precipitation and surface temperatures (Ropelewski & Halpert, 1987), which threaten vulnerable communities and ecosystems around the globe (Cane et al., 1994; Goddard & Gershunov, 2020; Holbrook et al., 2020). Much of ENSO research in recent decades has focused on the diversity of different characteristics of ENSO events (Capotondi et al., 2015) especially in spatial pattern, amplitude, and frequency. The diversity in the persistence of ENSO events and their impacts has not been explored in equivalent depth.

Persistent multi-year La Niña events are well-recognized phenomena (DiNezio et al., 2017; Ohba & Ueda, 2009; Okumura et al., 2011). The persistence of anomalies instigates additional economic and ecological consequences (Cole et al., 2002; Okumura, DiNezio, & Deser, 2017). On the other hand, modern observations have thus far indicated that El Niño events typically persist for a single year. The recent sequence of 2014–2015 and 2015–2016 El Niño events show that this is not a rule. The 2014–2016 El Niño event was both peculiarly persistent and anomalously strong. The 2014–2016 El Niño event prompted investigation into the mechanisms that could delay the termination of an El Niño event, identifying that late event initiation (Lee et al., 2020; Wu et al., 2019) and strengthened cross-equatorial meridional SST gradients (Lee et al., 2020). Others investigating ENSO diversity using a k-means clustering approach identified successive El Niño events as a unique cluster in observations, but noted that successive El Niño events can be

confused with central tropical Pacific events when using a small number of clusters (Wang et al., 2019). In fact, recent paleoclimate analysis has highlighted that several of the largest El Niño events over the late nineteenth and early twentieth century similarly featured this anomalous persistence (Sanchez et al., 2020). Other studies have described events of unusual persistence in the paleoarchives using varied terminology such as “prolonged,” “protracted,” “slow decay,” or “long lived” events (Allan & RosanneD’Arrigo, 1999; Allan et al., 2020; McGregor et al., 2013). For the purposes of our study, we consider these adjectives to be equivalent.

This study investigates the diversity of multi-year (successive) El Niño events in instrumental observations, a unique suite of Paleoclimate Modeling Intercomparison Project (PMIP3) Past1000/Last Millennium global climate models (GCM), and centuries of temperature sensitive coral archives from the central equatorial Pacific. We illustrate that this phenomenon may be more common than suggested from the perspective of relatively short observational records, and that there is large diversity in simulations amongst GCMs. We also show that these events have important implications for seasonal precipitation and surface temperature anomalies.

2. Data and Methods

2.1. Instrumental Observations

We examine observed sea surface temperature (SST) anomalies with the NOAA Extended Reconstruction version 5 (ERSSTv5; Huang et al., 2017). ERSSTv5 is a 2° resolution gridded monthly product spanning 1854–present to calculate Niño 3.4 indices. We validate results found in ERSSTv5 with other observational SST products; HADISST (Rayner et al., 2003), COBE SST2 (Hirahara et al., 2014), SODA2.2.4 (Giese & Ray, 2011) and Kaplan SST (Kaplan et al., 1998). We assess observed precipitation anomalies with the CPC Merged Analysis of Precipitation (CPC-CMAP; Xie & Arkin, 1997), which is a 2.5° gridded monthly product spanning 1979–present. We additionally consider the consistency of precipitation anomalies with twentieth Century reanalysis products: NOAA’s twentieth Century Reanalysis, 1851–2015 (Compo et al., 2011) and ERA twentieth Century Reanalysis, 1900–2010 (Poli et al., 2016). We also analyze observed surface temperature anomalies with the NASA GISS Surface Temperature Analysis version 4 (GISTEMP4; Hansen et al., 2010; Lenssen et al., 2019), a 2° gridded monthly product covering 1880–present.

2.2. Global Climate Model Simulations

We assess surface temperature and precipitation output from GCMs associated with the Coupled Model Intercomparison Project phase 5 (CMIP5; Taylor et al., 2012), Paleoclimate Model Intercomparison Project phase 3 (PMIP3) Past1000 runs (Braconnot et al., 2012); BCC-CSM1-1 (Wu et al., 2010), NCAR-CCSM4 (Landrum et al., 2013), CSIRO Mk3L-1–2 (Phipps et al., 2011), FGOALS-GL (Zhou et al., 2008), GISS-E2-R (Schmidt et al., 2014), HadCM3 (Gordon et al., 2000), IPSL-CM5-ALR (Hourdin et al., 2013), MIROC-ESM (Watanabe et al., 2011), MPI-ESM-P (Giorgetta et al., 2013; Jungclaus et al., 2013), MRI-CGCM3 (Yukimoto et al., 2012) and NCAR-CESM Last Millennium Ensemble (all-forcing and volcanic-only experiments; Otto-Bliesner et al., 2016). Analysis using the multi-model mean incorporates the single simulation from each of the various PMIP3 Past1000 experiments and the first full forcing ensemble member from the CESM Last Millennium Ensemble. The PMIP3 Past1000 experiments are a unique ensemble of experiments, each simulation was forced with the expected constraints arising from changes in volcanic, solar, land use change, orbital, and greenhouse gas forcing over the years 850–1850 (CMIP5/PMIP3 Past1000 experiments, Braconnot et al., 2012). Individual simulations within this suite of models can vary in the realism and skill with which they simulate mean climate and unforced climate variability, such as ENSO (Bellenger et al., 2014).

2.3. Central Equatorial Pacific Paleoclimate Archives

We assess historical Niño 3.4 behavior using oxygen isotope records from corals from the Line Islands in the central equatorial Pacific (Cobb et al., 2003; Dee et al., 2020; Sanchez et al., 2020), an archive highly correlated to the Niño 3.4 index (Figure S1, Cobb et al., 2003; Sanchez et al., 2020). The Line Island coral archives are the only long coral archives sourced directly from the central equatorial Pacific spanning the

last millennium. This record can document unusual ENSO phenomenon with a much higher fidelity than many of the other ENSO reconstructions using tree ring archives predominantly sourced from the mid-latitude continents that assume stationary ENSO teleconnection patterns through time. Furthermore, the oxygen isotopic composition of coral archives ($\delta^{18}\text{O}$) is controlled by variability SST and the oxygen isotopic composition of seawater ($\delta^{18}\text{Osw}$). $\delta^{18}\text{Osw}$ is modified by the processes of precipitation, evaporation, oceanic advection and upwelling (Fairbanks et al., 1997; Stevenson et al., 2015). The additional influence of $\delta^{18}\text{Osw}$ serves to heighten the variability observed in the central equatorial Pacific coral records, particularly at Palmyra (Russon et al., 2013), and this addition is most apparent during extreme El Niño events.

While coral archives allow us to extend analysis beyond the instrumental era, we acknowledge three caveats in this approach: (a) coral archives record climate variability from a single location, rather than the area averaged region (e.g., the Niño 3.4 index), and as such, the archives may be subject to local variability (b) the coral archives record variations in skeletal $\delta^{18}\text{O}$, a variable directly influenced by SST, but not identical, and (c) we impose a more rigorous threshold to the coral archives in identifying multi-year ENSO activity. As such, we do not expect the coral $\delta^{18}\text{O}$ index to be identical to instrumental Niño 3.4 variability. It is nonetheless a robust and indispensable perspective on past ENSO variability.

2.4. Identification of Multi-Year Events and Their Statistics

We first detrend all datasets by subtracting a thirty-year running mean to remove low-frequency variability in the background state. In the observational data and GCM output we calculate the Niño 3.4 index by calculating the area averaged SST anomaly over -5°S – 5°N , 170°W – 240°W , using annual averages defined as May through April.

As each data set in this study features a unique representation of ENSO with differences in overall amplitude of variability, we identify El Niño events using standardized anomalies (i.e., z-score) rather than SST anomalies. We identify single El Niño events as an event in which the annual anomaly reaches or exceeds 0.65 standard deviations for a single year. Multi-year El Niño events are classified as events that reach or exceed the same threshold for consecutive years. This specific threshold is somewhat arbitrary, but was identified to include the 2014–2016 El Niño event, a key motivation for this analysis. In this system of classification, we do not attempt to distinguish between successive El Niño events and single prolonged events. Most commonly, a multi-year event refers to a “double El Niño event,” or an event spans two consecutive years. In order to minimize false positives when identifying multi-year events in the multiple variables reflected in the $\delta^{18}\text{O}$ paleoclimate archives, we raise the threshold required for an El Niño event to 1 sigma in the annual average (in contrast to a 0.65 sigma threshold). Our results and overall conclusions are relatively insensitive to these details of the index. We find highly similar results when defining El Niño events in terms of their boreal winter (DJF) mean anomaly. We chose to use the annual average over the DJF seasonal anomaly because it facilitates comparison to paleoclimate archives.

Finally, we estimate the likelihood of two El Niño events appearing in consecutive years in each individual data set by using Monte Carlo methods to generate one million synthetic timeseries with randomized permutations. Each synthetic timeseries is designed to feature the same total length and the same unique total number of El Niño events (combined single and double events) as the true timeseries. We randomly reshuffle each timeseries of annual anomalies one million times and after each reshuffling, calculate the number of El Niño events that occur in consecutive years. We then create a histogram of the number of multi-year El Niño events found in the Monte Carlo experiment and can compare this to the true number of multi-year El Niño events in each product/simulation. If the observed number of double El Niño events falls inside of the distribution of synthetic double El Niño events, then multi-year events occur as often as expected and there is no obvious fingerprint of additional dynamical processes amplifying or dampening multi-event phenomena.

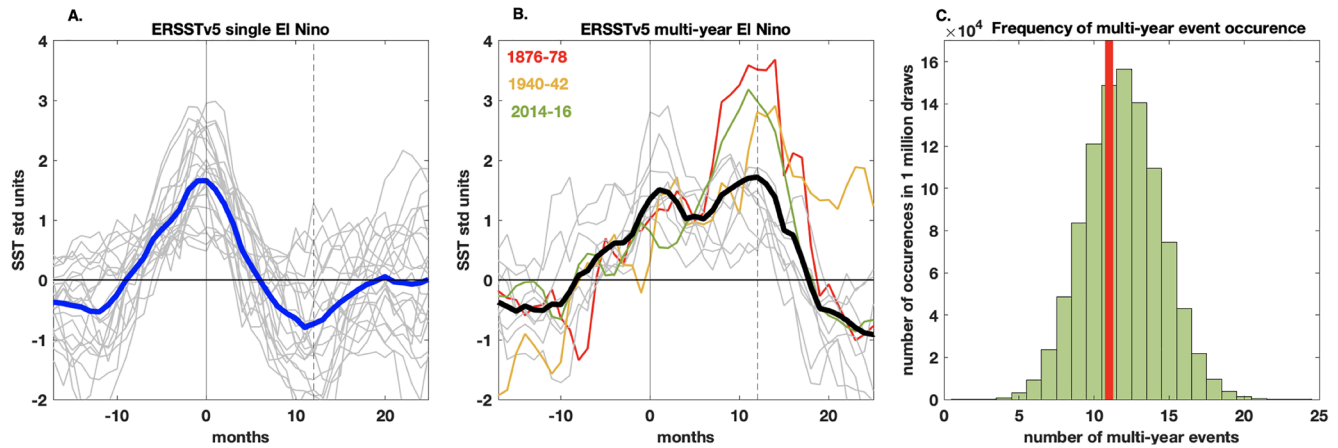


Figure 1. El Niño events in NOAA Extended Reconstruction version 5 (ERSSTv5). Individual single-year events (a) and multi-year events (b) are shown gray, denoted in Table S1. Event composites are illustrated by a bolded line for single (blue, (a)) and multi-year (black, (b)) events. X (0) corresponds to December of the first El Niño year. (c). The histogram of the number of multi-year events in synthetic time series (green), and the number of observed multi-year events (red bar).

3. Results

3.1. Multi-Year El Niños in Observations

Over the satellite era multi-year El Niño events have occurred less frequently than single year events, occurring only twice: during the 2014–2016 El Niño event and the 1986–1988 El Niño event (Figure 1b, Table S1). Multi-year events have also occurred semi-regularly over the late nineteenth and twentieth centuries, although many of these events occurred during periods when instrumental observations from the tropical Pacific were sparse (Figure 1b). Some of the largest El Niño events within the instrumental record are part of a protracted event that spans multiple years (e.g., 1876–1878, 1940–1942, 2014–2016, Sanchez et al., 2020). These results are fairly robust across other SST products. Over the satellite era, the varied observational products (ERSST, HadISST, COBE, SODA, Kaplan) are in 100% agreement (where applicable—SODA extends to 2010), however, during the early twentieth century, there are some minor differences between datasets in the classification of “multi-year” events (Table S2). Over the instrumental record, some of these events have had significant weather, ecological, and economic impacts around the world (e.g., Davis, 2002; Singh et al., 2018). The devastation associated with these events emphasizes the importance of understanding their dynamical origins as well as their associated risks.

How often should we expect multi-year El Niño events to occur in observations? Our results from reshuffling the observed events using the randomized permutations (Figure 1c) indicate that multi-year events occur about as often as statistically expected. Therefore, any dynamical processes that may modify multi-year events do not result in a distinctly different probability distribution over the instrumental era. We will revisit this idea in the following sections.

3.2. Multi-Year El Niños in Paleoclimate Archives and GCMs

Multi-year events are not only found in the instrumental record; we find evidence of similarly protracted events in central equatorial Pacific coral $\delta^{18}\text{O}$ records (Figure 2m). Furthermore, all of the climate models considered are capable of resolving multi-year El Niño events (Figures 2b–2l), despite the well documented variation in simulation of the tropical Pacific within the CMIP5 experiments (Bellenger et al., 2014). However, these varied sources express great diversity in the mean characteristics of the multi-year El Niño events. We highlight several here: (a) blended versus distinct events, (b) event magnitude, (c) initiation timing, and (d) state of ENSO following the multi-year event.

Multiple model composites resolve distinct peaks related to each El Niño event (CCSM, CESM, CSIRO, HAD, paleoarchives), while others blend the multi-year peaks together as a single long event (e.g., FGOALS). In several multi-model composites, the relative amplitude of the first and second El Niño events are of

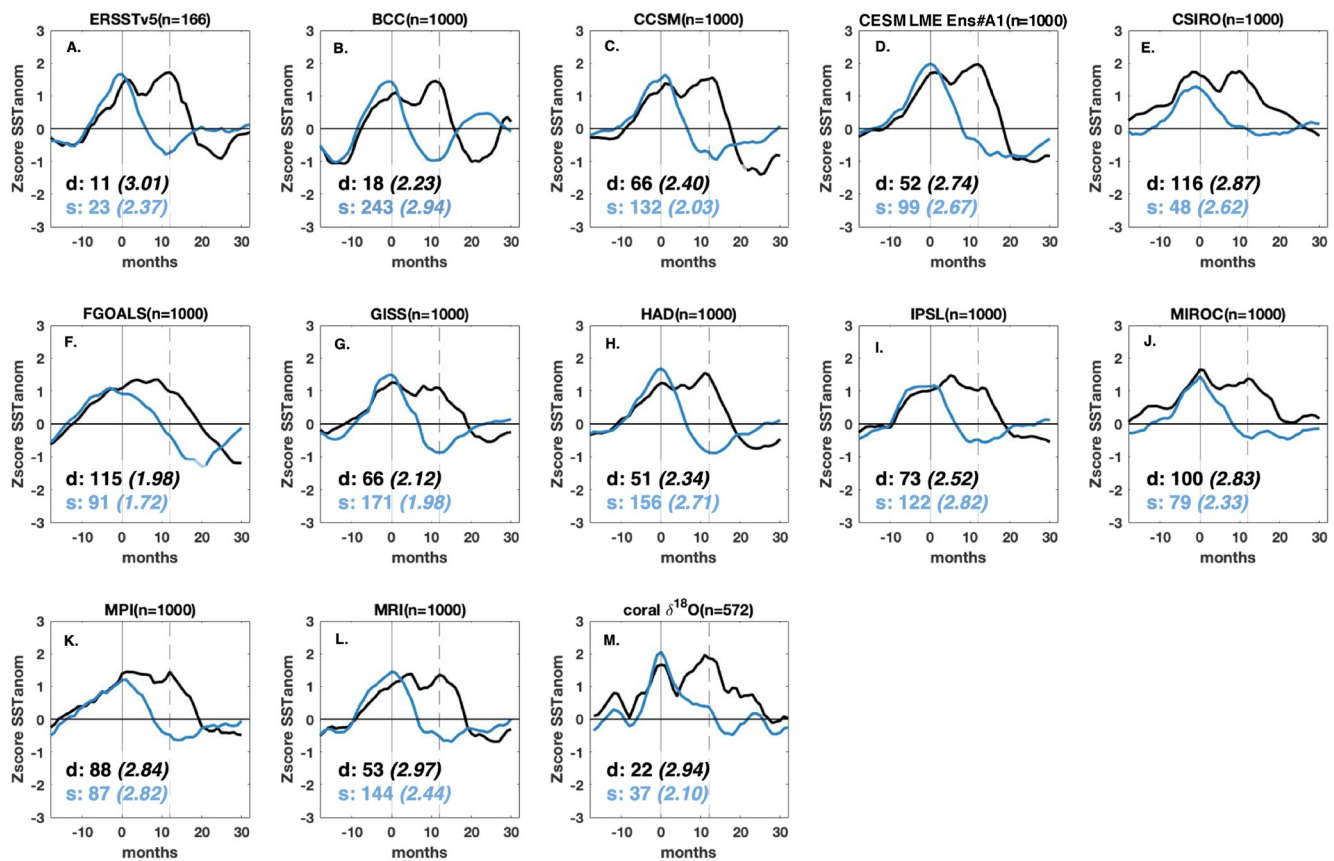


Figure 2. Composite monthly progression of El Niño events in the observations, climate models, and central equatorial Pacific paleoarchives. Zscored anomalies are plotted, X (0) corresponds to December of the first El Niño year, the dashed X (11) corresponds to the second. The single El Niño event mean (blue) and multi-year El Niño event mean (black) are plotted for each simulation, n denotes the number of years available. The number of each type of event is indicated in the bottom left corner for single (“s,” blue) and multi-year (“d,” black) events. The magnitude of the 98th percentile El Niño event for each type of El Niño event is provided in parentheses.

differing magnitudes. In many models, the first El Niño event is of smaller amplitude than the second event (e.g., BCC, HAD, CCSM, CESM). When contrasting multi-year events with single year events, differences in the timing of event initiation are also apparent, as described in Wu et al. (2021). In most of the model composites the multi-year El Niño event is initiated several months later than the average single El Niño event, but the magnitude of the lag is model dependent. Similar to traditional, single El Niño events, in the majority of models assessed, the average multi-year event is followed by a cool La Niña-like state. In both multi-year events and single year events, the DJF following the termination of the El Niño features multi-model composite of SST anomalies of ~ -0.50 standard deviations.

In any given 1000-year simulation of the tropical Pacific, how likely is it that two El Niño events will occur in succession? Do individual climate models/archives fall within this range of expectations? Multi-year events occur well within the range expected from the randomized permutation experiments in many of these models, but not all (Figure S2). The number of actual multi-year event occurrences are well outside of the bounds of expectation in two models: the BCC (below expectation) and CSIRO (above expectation) models. This is likely due to differences in model physics, suggesting that some underlying model bias or dynamics influences the frequency of the occurrence of these events. Interestingly, the paleorecord indicates a higher frequency of multi-year El Niño events than the instrumental record, despite the stricter event criterion (Figures S21–S2n). This distinction is due to the variability recorded earlier in the millennium, the modern portion of the paleorecord demonstrates variability highly similar to that found in the instrumental record. While some of this may be due to the difference in the variable examined (local coral $\delta^{18}\text{O}$ vs. area averaged SST), this is evidence that the multi-year El Niño events may have been more common at other points over the last millennium.

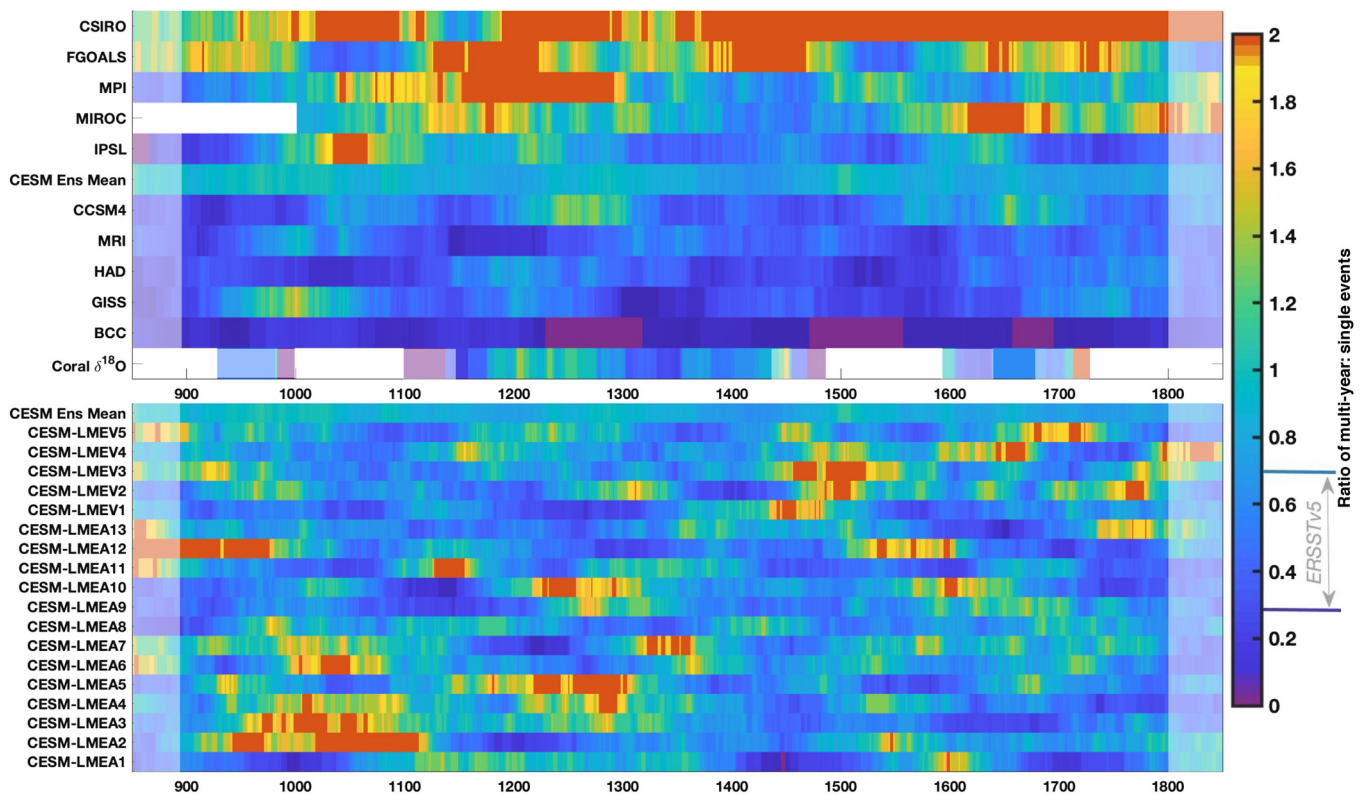


Figure 3. Heat map of the frequency of multi-year El Niño events relative to the frequency of single events. For each datasource, the ratio of the number of multi-year events relative to the number of single El Niño events is calculated using a centered 100 year moving window. The model/data set identification is on the left y-axis. The range of values in the instrumental record is illustrated next to the colorbar. The centered windowing approach limits the evaluation of a 100-year averaged ratio near the simulation endpoints; ratios estimated within the 50 years closest to the start/end of the simulation do not consider a full 100-year period and are indicated with shading.

3.3. Variability of Multi-Year Events

Based on the three perspectives of ENSO variability, multi-year events occur at a wide range of frequencies. In the observational record, the frequency spans 5–9 events/century, when using complete 100-year windows. In climate models, the frequency spans 0–18 events/century (BCC and CSIRO, respectively). In order to distinguish multi-year El Niño activity from total ENSO variability, we compare the ratio of the number of multi-year events to the number of single events (Figure 3). Across the various models, there is vast diversity in the simulated variability. For example, BCC has very little multi-year ENSO activity, while CSIRO features a higher proportion of multi-year events to single events over the second half of the last millennium. Additionally, there are high amounts of internal variability found within individual model simulations. Intercentennial and interdecadal variability in the frequency of multi-year El Niño events is a common feature throughout each of the climate models and paleoarchives considered.

Within the instrumental era, the range of variability exhibited over any continuous 100-year period is about 0.3–0.7 double to single events. However, the instrumental era features variations in radiative forcing distinct from those simulated in the Past1000 experiments so differences in frequency of occurrence could be influenced by differences in the climate mean state. We can examine the sensitivity of the frequency of multi-year events in response to these changes in radiative forcing by comparing the various Past1000 experiments, each simulation run with the same forcing constraints (Braconnot et al., 2012). If the ratio of double to single El Niño events was sensitive to historical variations in radiative forcing, we would expect to find common periods of heightened activity in Figure 3, particularly in the CESM Last Millennium Ensemble simulations as each simulation is subject to the same model physics. We find no evidence that the frequency of multi-year El Niño events have responded to forced change over the last millennium.

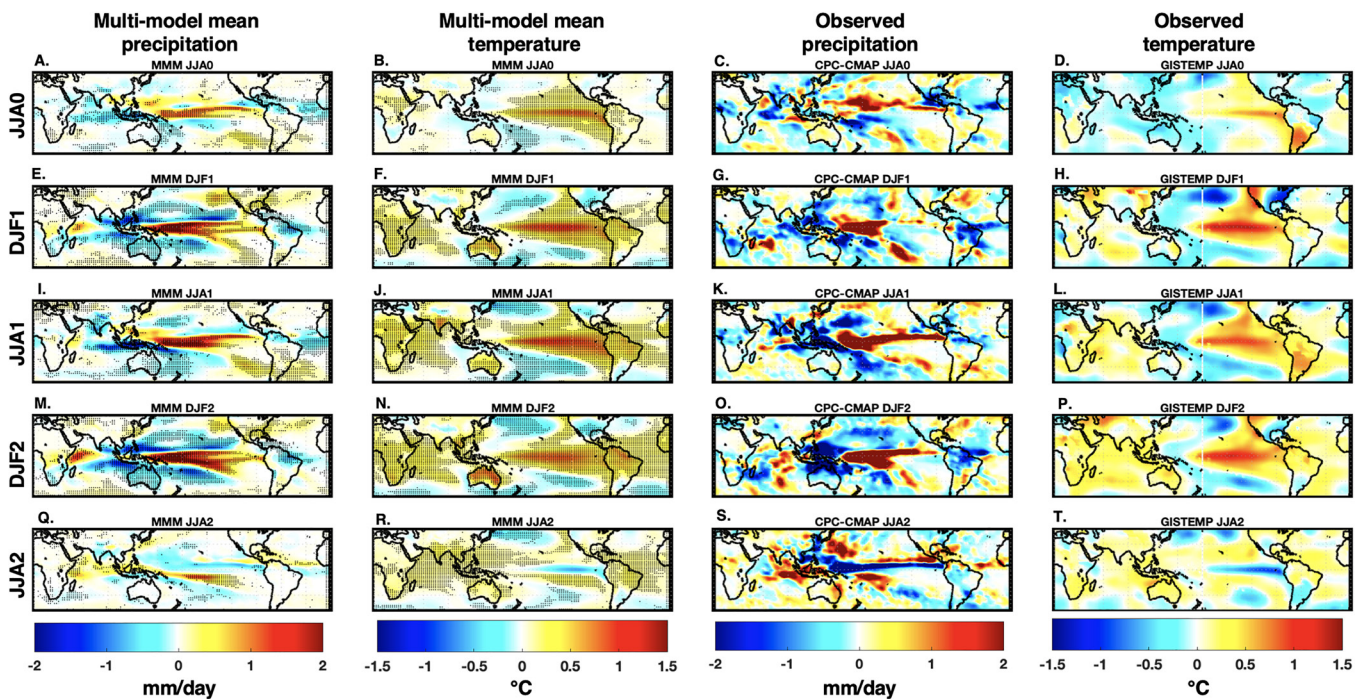


Figure 4. Composite precipitation and surface temperature anomalies during the multi-year El Niño events. Precipitation anomalies are plotted for JJA and DJF in a multi-year event sequence using the Past1000/Last Millennium multi-model composite (a, e, i, m, and q) and the CPC Merged Analysis of Precipitation (CPC-CMAP) composite (c, g, k, o, and s), respectively. Surface temperature anomalies are plotted for the multi-year event sequence using the Past1000/Last Millennium multi-model composite (b, f, j, n, and r) and the GISS Surface Temperature Analysis version 4 (GISTEMP4) composite (d, h, l, p, and t), respectively. Stippling indicates that 9 of the 11 climate models represented in this multi-model composite feature the same sign mean anomaly in consecutive years.

3.4. Impacts of Multi-Year Events

We consider the impact of multi-year El Niño events on seasonal precipitation and surface temperature anomalies for the boreal winter and summer months in instrumental observations (Figures 4a, 4c, 4e and 4g) and the multi-model mean of the Past1000/Last Millennium simulations (Figures 4b, 4d, 4f and 4h). Individual results for each respective season and model/reanalysis product can be found in Figures S3–S7. Even when considering single-year El Niño events, impacts can be quite diverse due to modification from unforced low frequency variability (e.g., Feba et al., 2018; Tejavath et al., 2019). Both surface temperature and precipitation impacts associated with multi-year events are similar to the mean of traditional, single year ENSO impacts (Figure S8); these impacts chiefly differ in that they arise in consecutive seasons. However, in observations and many individual climate models, DJF SST anomalies are strongest in the central tropical Pacific, which may be an important clue to understanding the dynamical mechanisms behind these events.

Across the tropics, regions exposed to high magnitude ENSO impacts may be even more vulnerable to severe consequences as a result of the consecutive years of drought or pluvial for example, Allan et al. (2020) (Figure 4). Furthermore, multi-year events are often followed by a La Niña (Figure 2). La Niña events further have considerable impacts on seasonal precipitation and surface temperature anomalies (Glantz, 2002). We hypothesize that such extreme changes could prompt local “whiplash events” (Swain et al., 2018, e.g., two extreme dry/wet seasons followed by a wet/dry season), enhancing the severity of a multi-year El Niño event sequence.

Multi-year events are not only unusual for their persistence, but can also stand out due to their magnitude. For any given El Niño event, a single or multi-year event may be of comparable magnitude. However, in the instrumental record, multi-year events are among the largest observed, for example, 1877–1878, 1941–1942, 2015–2016 (Figure 1, Sanchez et al., 2020). We compare the magnitude of the largest events by calculating the magnitude of 98th percentile multi-year (double) and single events. In 8 of the 11 models considered,

the 98th percentile of double event sequences were larger than the 98th percentile event in single El Niño events by 0.12 standard deviations on average (Figure 2, Table S3). In observations, the 98th percentile of a multi-year event exceeds that of a single year event by 0.64 standard deviations, and by 0.83 standard deviations in the paleoarchives. A similar relationship holds if considering 90th percentile events (Table S3). If we consider the largest 2% of all El Niño events in each of the last millennium simulations and observational products, the majority of the largest events were associated with a double event (57%, Table S3). This fraction varies considerably amongst individual models. In 5 of the 11 models considered, >75% of the largest 2% of total events are multi-year events. In both instrumental observations and paleoclimate archives, the vast majority of the largest 2% of events were multi-year phenomena. It is therefore possible that a physical mechanism unique to formation of double events encourages the amplified growth of such events.

4. Discussion and Conclusion

ENSO variability features a vast range of internal variability at interdecadal and intercentennial timescales (Capotondi et al., 2015; Cobb et al., 2013; Karaukas et al., 2012; Wittenberg, 2009). Here, we consider the diversity in the persistence of El Niño events. We find consistent evidence in instrumental observations, paleoclimate archives, and GCMs that multi-year El Niño events are an emergent feature of the climate system. Furthermore, we find evidence that these events may be more common than reflected over the satellite era.

Even within the instrumental record, the frequency with which multi-year El Niño events occur has varied, featuring relatively low activity since the mid twentieth century. We find evidence that the present climate may be in a period of relatively infrequent multi-year events; paleoarchives indicate that periods of frequent multi-year El Niño events (relative to single El Niño events) have occurred semi-regularly throughout the last millennium. The CMIP5 Past1000 and CESM Last Millennium Ensemble experiments further demonstrate unforced interdecadal and intercentennial variability in the frequency of multi-year event occurrence.

It is still unknown what dynamical mechanisms are most important in the persistence of a multi-year El Niño event. The limited instrumental record and the diversity of tropical Pacific dynamics in model simulations inhibit a clear assessment of potential mechanisms. Of the models considered, there are a variety of potentially important features that may influence the persistence of El Niño events and the amplitude of multi-year events: the timing of event initiation (Wu et al., 2021), the degree of decay after the first event (e.g., a blended event vs. two distinct events), the spatial pattern of SST anomalies during the event, and the development of the anomaly patterns with regard to ENSO flavors. The background state of the global ocean or atmosphere may precondition the tropical Pacific for these unusually persistent events. Okumura, Sun, and Wu (2017) found that multi-year El Niño events occur more frequently in NCAR's CCSM4 when low frequency variability in the tropical Pacific has a warmer background state. Nonetheless, there is a consensus from the GCMs, paleoclimate archives and instrumental observations that multi-year El Niño events are among the largest El Niños simulated. All models considered here provide evidence that these multi-year events can instigate persistent impacts on seasonal precipitation and surface temperature anomalies in regions particularly vulnerable to ENSO impacts.

Finally, it is not known if or how anthropogenic climate change may influence the development of multi-year El Niño activity, or modulate the associated impacts. Anthropogenic change may already be influencing the spatial pattern of ENSO anomalies from more eastern Pacific to central Pacific events (Ashok et al., 2007; Freund et al., 2019; Kim & Yu, 2012; Yeh et al., 2009). Several studies have suggested that mechanisms critical for the development of central Pacific El Niño events may be related to the development of multi-year El Niño events (Kim & Yu, 2020; Sanchez et al., 2020; Wang et al., 2019), thus a changing frequency of central Pacific events may have implications for the development of multi-year El Niño events. Finally, ENSO impacts may be more devastating in the future (Fasullo et al., 2018; Stevenson, 2012), particularly regarding precipitation impacts (Power et al., 2013; Seager et al., 2012; Yun et al., 2021). If true, it is possible that these large, multi-year El Niño events may be an important part of that future.

Data Availability Statement

Data for our instrumental-based analysis were provided by several sources: NOAA Extended Reconstruction Sea Surface Temperatures version 5 (Huang et al., 2017, <https://www.ncdc.noaa.gov/data-access/marineocean-data/extended-reconstructed-sea-surface-temperature-ersst-v5>), NOAA/OAR/ESRL PSL CPC Merged Analysis of Precipitation (Xie & Arkin, 1997, <https://psl.noaa.gov/data/gridded/data.cmap.html>), and NASA GISS Surface Temperature Analysis version 4 (Lenssen et al., 2019, <https://data.giss.nasa.gov/gistemp/>). Data for our reanalysis-based precipitation analysis were provided by NOAA-CIRES Twentieth Century Reanalysis version 2C (Compo et al., 2011, https://psl.noaa.gov/data/gridded/data.20thC_ReanV2c.html) and ERA Twentieth Century Reanalysis (Poli et al., 2016, <https://www.ecmwf.int/en/forecasts/datasets/reanalysis-datasets/era-20c>).

Acknowledgments

S.C. Sanchez was funded by the University of Colorado Chancellor's Postdoctoral Fellowship. The authors acknowledge the individual data sources that made this analysis possible. The authors acknowledge the NOAA National Climate Data Center Paleoclimate database for our paleoclimate archive data analysis. Coral records from the Line Islands are published in the following studies: Sanchez et al., 2020 (<https://www.ncdc.noaa.gov/paleo-search/study/30493>), Dee et al., 2020 (<https://www.ncdc.noaa.gov/paleo-search/study/27490>), and Cobb et al., 2003 (<https://www.ncdc.noaa.gov/paleo-search/study/1875>). Finally, the authors would like to acknowledge the CMIP5/PMIP3 project activity, with governance provided by the World Climate Research Program's (WCRP) Data Advisory Council (WDAC), and model output hosted by the Earth System Grid Federation- Department of Energy Lawrence Livermore National Lab node. The authors acknowledge the individual CMIP5/PMIP3 Past1000 models used in this analysis: BCC-CSM1-1 (Wu et al., 2010), NCAR-CCSM4 (Landrum et al., 2013), CSIRO Mk3L-1-2 (Phipps et al., 2011), FGOALS-GL (Zhou et al., 2008), GISS-E2-R (Schmidt et al., 2014), HadCM3 (Gordon et al., 2000), IPSL-CM5-ALR (Hourdin et al., 2013), MIROC-ESM (Watanabe et al., 2011), MPI-ESM-P (Giorgetta et al., 2013; Jungclauss et al., 2013), MRI-CGCM3 (Yukimoto et al., 2012); model output for each experiment can be found at <https://esgf-node.llnl.gov/projects/esgf-llnl/>. The authors also acknowledge NCAR's CESM Last Millennium Ensemble (Otto-Bliesner et al., 2016), data can be accessed here, <https://www.earthsystemgrid.org/dataset/ucar.cgd.cesm4.cesmLME.html>. The randomization experiments were conducted using MATLAB 2021A.

References

- Allan, R. J., Gergis, J., & D'Arrigo, R. D. (2020). Placing the AD 2014–2016 'protracted' El Niño episode into a long-term context. *The Holocene*, 30(1), 90–105. <https://doi.org/10.1177/0959683619875788>
- Allan, R. J., & RosanneD'Arrigo, D. (1999). 'Persistent' ENSO sequences: How unusual was the 1990-1995 El Niño? *The Holocene*, 9(1), 101–118. <https://doi.org/10.1191/095968399669125102>
- Ashok, K., Behera, S. K., Rao, S. A., Weng, H., & Yamagata, T. (2007). El Niño Modoki and its possible teleconnection. *Journal of Geophysical Research*, 112, C11007. <https://doi.org/10.1029/2006jc003798>
- Bellenger, H., Guilyardi, É., Leloup, J., Lengaigne, M., & Vialard, J. (2014). ENSO representation in climate models: From CMIP3 to CMIP5. *Climate Dynamics*, 42(7), 1999–2018. <https://doi.org/10.1007/s00382-013-1783-z>
- Bjerknes, J. (1969). Atmospheric teleconnections from the equatorial Pacific. *Monthly Weather Review*, 97(3), 163–172. [https://doi.org/10.1175/1520-0493\(1969\)097<0163:atftep>2.3.co;2](https://doi.org/10.1175/1520-0493(1969)097<0163:atftep>2.3.co;2)
- Braconnot, P., Harrison, S. P., Kageyama, M., Bartlein, P. J., Masson-Delmotte, V., Abe-Ouchi, A., et al. (2012). Evaluation of climate models using palaeoclimatic data. *Nature Climate Change*, 2, 417–424. <https://doi.org/10.1038/nclimate1456>
- Cane, M. A., Eshel, G., & Buckland, R. W. (1994). Forecasting Zimbabwean maize yield using eastern equatorial Pacific sea surface temperature. *Nature*, 370(6486), 204–205.
- Capotondi, A., Wittenberg, A. T., Newman, M., Di Lorenzo, E., Yu, J.-Y., Braconnot, P., et al. (2015). Understanding ENSO diversity. *Bulletin of the American Meteorological Society*, 96(6), 921–938. <https://doi.org/10.1175/bams-d-13-00117.1>
- Cobb, K. M., Charles, C. D., Cheng, H., & Edwards, R. L. (2003). El Niño/Southern Oscillation and tropical Pacific climate during the last millennium. *Nature*, 424(6946), 271–276.
- Cobb, K. M., Westphal, N., Sayani, H. R., Watson, J. T., Lorenzo, E. D., Cheng, H., et al. (2013). Highly variable El Niño–Southern Oscillation throughout the Holocene. *Science*, 339, 67–70. <https://doi.org/10.1126/science.1228246>
- Cole, J. E., Overpeck, J. T., & Cook, E. R. (2002). Multiyear La Niña events and persistent drought in the contiguous United States. *Geophysical Research Letters*, 29(13), 25-1–25-4. <https://doi.org/10.1029/2001gl013561>
- Compo, G. P., Whitaker, J. S., Sardeshmukh, P. D., Matsui, N., Allan, R. J., Yin, X., et al. (2011). The twentieth century reanalysis project. *Quarterly Journal of the Royal Meteorological Society*, 137, 1–28. <https://doi.org/10.1002/qj.776>
- Davis, M. (2002). *Late Victorian holocausts: El Niño famines and the making of the third world*. Verso Books.
- Dee, S. G., Cobb, K. M., Emile-Geay, J., Ault, T. R., Edwards, R. L., Cheng, H., & Charles, C. D. (2020). No consistent ENSO response to volcanic forcing over the last millennium. *Science*, 367, 1477–1481. <https://doi.org/10.1126/science.aax2000>
- DiNezio, P. N., Deser, C., Okumura, Y., & Karspeck, A. (2017). Predictability of 2-year La Niña events in a coupled general circulation model. *Climate Dynamics*, 49(11), 4237–4261. <https://doi.org/10.1007/s00382-017-3575-3>
- Fairbanks, R. G., Evans, M. N., Rubenstone, J. L., Mortlock, R. A., Broad, K., Moore, M. D., & Charles, C. D. (1997). Evaluating climate indices and their geochemical proxies measured in corals. *Coral Reefs*, 16(1), S93–S100. <https://doi.org/10.1007/s003380050245>
- Fasullo, J. T., Otto-Bliesner, B. L., & Stevenson, S. (2018). ENSO's changing influence on temperature, precipitation, and wildfire in a warming climate. *Geophysical Research Letters*, 45(17), 9216–9225. <https://doi.org/10.1029/2018gl079022>
- Feba, F., Ashok, K., & Ravichandran, M. (2019). Role of changed Indo-Pacific atmospheric circulation in the recent disconnect between the Indian summer monsoon and ENSO. *Climate Dynamics*, 52(3), 1461–1470.
- Freund, M. B., Henley, B. J., Karoly, D. J., McGregor, H. V., Abram, N. J., & Dommenget, D. (2019). Higher frequency of Central Pacific El Niño events in recent decades relative to past centuries. *Nature Geoscience*, 12(6), 450–455. <https://doi.org/10.1038/s41561-019-0353-3>
- Giese, B. S., & Ray, S. (2011). El Niño variability in simple ocean data assimilation (SODA), 1871–2008. *Journal of Geophysical Research*, 116, C02024. <https://doi.org/10.1029/2010jc006695>
- Giorgetta, M. A., Jungclauss, J., Reick, C. H., Legutke, S., Bader, J., Bottinger, M., et al. (2013). Climate and carbon cycle changes from 1850 to 2100 in MPI-ESM simulations for the coupled model intercomparison project phase 5. *Journal of Advances in Modeling Earth Systems*, 5, 572–597. <https://doi.org/10.1002/jame.20038>
- Glantz, M. (2002). *La Niña and its impacts: Facts and speculation*. United Nations University (UNU).
- Goddard, L., & Gershunov, A. (2020). Impact of El Niño on weather and climate extremes. In *El Niño Southern oscillation in a changing climate* (pp. 361–375). <https://doi.org/10.1002/9781119548164.ch16>
- Gordon, C., Cooper, C., Senior, C. A., Banks, H., Gregory, J. M., Johns, T. C., et al. (2000). The simulation of SST, sea ice extents and ocean heat transports in a version of the Hadley Centre coupled model without flux adjustments. *Climate Dynamics*, 16, 147–168. <https://doi.org/10.1007/s003820050010>
- Hansen, J., Ruedy, R., Sato, M., & Lo, K. (2010). Global surface temperature change. *Reviews of Geophysics*, 48, RG4004. <https://doi.org/10.1029/2010rg000345>
- Hirahara, S., Ishii, M., & Fukuda, Y. (2014). Centennial-scale sea surface temperature analysis and its uncertainty. *Journal of Climate*, 27, 57–75. <https://doi.org/10.1175/jcli-d-12-00837.1>
- Holbrook, N. J., Claar, D. C., Hobday, A. J., McInnes, K. L., Oliver, E. C. J., Gupta, A. S., et al. (2020). ENSO-Driven ocean extremes and their ecosystem impacts. In *El Niño Southern oscillation in a changing climate* (pp. 409–428). <https://doi.org/10.1002/9781119548164.ch18>

- Hourdin, F., Foujols, M.-A., Codron, F., Guemas, V., Dufresne, J.-L., Bony, S., et al. (2013). Impact of the LMDZ atmospheric grid configuration on the climate and sensitivity of the IPSL-CM5A coupled model. *Climate Dynamics*, *40*, 2167–2192. <https://doi.org/10.1007/s00382-012-1411-3>
- Huang, B., Thorne, P. W., Banzon, V. F., Boyer, T., Chepurin, G., et al. (2017). Extended reconstructed sea surface temperature version 5 (ERSSTv5), upgrades, validations, and intercomparisons. *Journal of Climate*, *30*, 8179–8205. <https://doi.org/10.1175/JCLI-D-16-0836.1>
- Jungclauss, J. H., Fischer, N., Haak, H., Lohmann, K., Marotzke, J., Matei, D., et al. (2013). Characteristics of the ocean simulations in the Max Planck Institute Ocean Model (MPIOM) the ocean component of the MPI-Earth system model. *Journal of Advances in Modeling Earth Systems*, *5*, 422–446. <https://doi.org/10.1002/jame.20023>
- Kaplan, A., Cane, M. A., Kushnir, Y., Clement, A. C., Blumenthal, M. B., & Rajagopalan, B. (1998). Analyses of global sea surface temperature 1856–1991. *Journal of Geophysical Research*, *103*(C9), 18567–18589. <https://doi.org/10.1029/97jc01736>
- Karnauskas, K. B., Smerdon, J. E., Seager, R., & González-Rouco, J. F. (2012). A Pacific centennial oscillation predicted by coupled GCMs. *Journal of Climate*, *25*(17), 5943–5961. <https://doi.org/10.1175/jcli-d-11-00421.1>
- Kim, J.-W., & Yu, J.-Y. (2020). Understanding reintensified multiyear El Niño events. *Geophysical Research Letters*, *47*, e2020GL087644. <https://doi.org/10.1029/2020gl087644>
- Kim, S. T., & Yu, J.-Y. (2012). The two types of ENSO in CMIP5 models. *Geophysical Research Letters*, *39*, L11704. <https://doi.org/10.1029/2012GL052006>
- Landrum, L., Otto-Bliesner, B. L., Wahl, E. R., Conley, A., Lawrence, P. J., Rosenbloom, N., & Teng, H. (2013). Last millennium climate and its variability in CCSM4. *Journal of Climate*, *26*, 1085–1111. <https://doi.org/10.1175/JCLI-D-11-00326.1>
- Lee, C.-W., Tseng, Y.-H., Sui, C.-H., Zheng, F., & Wu, E.-T. (2020). Characteristics of the prolonged El Niño events during 1960–2020. *Geophysical Research Letters*, *47*, e2020GL088345. <https://doi.org/10.1029/2020gl088345>
- Lenssen, N., Schmidt, G., Hansen, J., Menne, M., Persin, A., Ruedy, R., & Zyss, D. (2019). Improvements in the GISTEMP uncertainty model. *Journal of Geophysical Research - D: Atmospheres*, *124*(12), 6307–6326. <https://doi.org/10.1029/2018JD029522>
- McGregor, S., Timmermann, A., England, M. H., Elison Timm, O., & Wittenberg, A. T. (2013). Inferred changes in El Niño–Southern Oscillation variance over the past six centuries. *Climate of the Past*, *9*, 2269–2284. <https://doi.org/10.5194/cp-9-2269-2013>
- Ohba, M., & Ueda, H. (2009). Role of nonlinear atmospheric response to SST on the asymmetric transition process of ENSO. *Journal of Climate*, *22*(1), 177–192. <https://doi.org/10.1175/2008jcli2334.1>
- Okumura, Y. M., DiNezio, P., & Deser, C. (2017). Evolving impacts of multiyear La Niña events on atmospheric circulation and US drought. *Geophysical Research Letters*, *44*(22), 11–614. <https://doi.org/10.1002/2017gl075034>
- Okumura, Y. M., Ohba, M., Deser, C., & Ueda, H. (2011). A proposed mechanism for the asymmetric duration of El Niño and La Niña. *Journal of Climate*, *24*(15), 3822–3829. <https://doi.org/10.1175/2011jcli3999.1>
- Okumura, Y. M., Sun, T., & Wu, X. (2017). Asymmetric modulation of El Niño and La Niña and the linkage to tropical Pacific decadal variability. *Journal of Climate*, *30*, 4705–4733. <https://doi.org/10.1175/jcli-d-16-0680.1>
- Otto-Bliesner, B. L., Brady, E. C., Fasullo, J., Jahn, A., Landrum, L., Stevenson, S., et al. (2016). Climate variability and change since 850 CE: An ensemble approach with the community earth system model. *Bulletin of the American Meteorological Society*, *97*(5), 735–754. <https://doi.org/10.1175/bams-d-14-00233.1>
- Phipps, S. J., Rotstayn, L. D., Gordon, H. B., Roberts, J. L., Hirst, A. C., & Budd, W. F. (2011). The CSIRO Mk3L climate system model version 1.0–Part 1: Description and evaluation. *Geoscientific Model Development*, *4*(2), 483–509. <https://doi.org/10.5194/gmd-4-483-2011>
- Poli, P., Hersbach, H., Dee, D. P., Paul, B., Vitart, F., Simmons, A. J., et al. (2016). ERA-20C: An atmospheric reanalysis of the twentieth century. *Journal of Climate*, *29*(11), 4083–4097. <https://doi.org/10.1175/jcli-d-15-0556.1>
- Power, S., Delage, F., Chung, C., Kociuba, G., & Keay, K. (2013). Robust twenty-first-century projections of El Niño and related precipitation variability. *Nature*, *502*(7472), 541–545. <https://doi.org/10.1038/nature12580>
- Rayner, N. A., Parker, D. E., Horton, E. B., Folland, C. K., Alexander, L. V., Rowell, D. P., et al. (2003). Global analyses of sea surface temperature, sea ice, and night marine air temperature since the late nineteenth century. *Journal of Geophysical Research*, *108*, 4407. <https://doi.org/10.1029/2002JD002670>
- Ropelewski, C. F., & Halpert, M. S. (1987). Global and regional scale precipitation patterns associated with the El Niño/Southern Oscillation. *Monthly Weather Review*, *115*(8), 1606–1626. [https://doi.org/10.1175/1520-0493\(1987\)115<1606:garspp>2.0.co;2](https://doi.org/10.1175/1520-0493(1987)115<1606:garspp>2.0.co;2)
- Russon, T., Tudhope, A. W., Hegerl, G. C., Collins, M., & Tindall, J. (2013). Inter-annual tropical Pacific climate variability in an isotope-enabled CGCM: Implications for interpreting coral stable oxygen isotope records of ENSO. *Climate of the Past*, *9*(4), 1543–1557. <https://doi.org/10.5194/cp-9-1543-2013>
- Sanchez, S. C., Westphal, N., Haug, G. H., Cheng, H., Edwards, R. L., Schneider, T., & Charles, C. D. (2020). A continuous record of central tropical Pacific climate since the midnineteenth century reconstructed from fanning and palmyra island corals: A case study in coral data reanalysis. *Paleoceanography and Paleoclimatology*, *35*(8), e2020PA003848. <https://doi.org/10.1029/2020pa003848>
- Schmidt, G. A., Kelley, M., Nazarenko, L., Ruedy, R., Russell, G. L., Aleinov, I., et al. (2014). Configuration and assessment of the GISS ModelE2 contributions to the CMIP5 archive. *Journal of Advances in Modeling Earth Systems*, *6*, 141–184. <https://doi.org/10.1002/2013MS000265>
- Seager, R., Naik, N., & Vogel, L. (2012). Does global warming cause intensified interannual hydroclimate variability? *Journal of Climate*, *25*(9), 3355–3372. <https://doi.org/10.1175/jcli-d-11-00363.1>
- Singh, D., Seager, R., Benjamin, I., Cook, C. A., Ting, M., et al. (2018). Climate and the global famine of 1876–78. *Journal of Climate*, *31*(23), 9445–9467. <https://doi.org/10.1175/jcli-d-18-0159.1>
- Stevenson, S., Powell, B. S., Merrifield, M. A., Cobb, K. M., Nusbaumer, J., & Noone, D. (2015). Characterizing seawater oxygen isotopic variability in a regional ocean modeling framework: Implications for coral proxy records. *Paleoceanography*, *30*(11), 1573–1593. <https://doi.org/10.1002/2015pa002824>
- Stevenson, S. L. (2012). Significant changes to ENSO strength and impacts in the twenty-first century: Results from CMIP5. *Geophysical Research Letters*, *39*, L17703. <https://doi.org/10.1029/2012gl052759>
- Swain, D. L., Langenbrunner, B., David Neelin, J., & Hall, A. (2018). Increasing precipitation volatility in twenty-first-century California. *Nature Climate Change*, *8*(5), 427–433. <https://doi.org/10.1038/s41558-018-0140-y>
- Taylor, K. E., Stouffer, S. R., & Meehl, A. G. (2012). An overview of CMIP5 and the experiment design. *Bulletin of the American Meteorological Society*, *93*, 485–498.
- Tejavath, C. T., Ashok, K., Chakraborty, S., & Ramesh, R. (2019). A PMIP3 narrative of modulation of ENSO teleconnections to the Indian summer monsoon by background changes in the Last Millennium. *Climate Dynamics*, *53*(5), 3445–3461.
- Wang, B., Luo, X., Yang, Y.-M., Sun, W., Cai, W., Yeh, S.-W., et al. (2019). Historical change of El Niño properties sheds light on future changes of extreme El Niño. *Proceedings of the National Academy of Sciences*, *116*(45), 22512–22517. <https://doi.org/10.1073/pnas.1911130116>

- Watanabe, S., Hajima, T., Sudo, K., Nagashima, T., Takemura, T., & Okajima, H., et al. (2011). MIROC-ESM 2010: Model description and basic results of CMIP5-20c3m experiments. *Geoscientific Model Development*, 4(4), 845–872. <https://doi.org/10.5194/gmd-4-845-2011>
- Wittenberg, A. T. (2009). Are historical records sufficient to constrain ENSO simulations? *Geophysical Research Letters*, 36(12), L12702. <https://doi.org/10.1029/2009gl038710>
- Wu, T., Yu, R., Zhang, F., Wang, Z., Dong, M., & Wang, L., et al. (2010). The Beijing climate center atmospheric general circulation model: Description and its performance for the present-day climate. *Climate Dynamics*, 34, 123–147. <https://doi.org/10.1007/s00382-008-0487-2>
- Wu, X., Okumura, Y. M., & DiNezio, P. N. (2019). What controls the duration of El Niño and La Niña events? *Journal of Climate*, 32(18), 5941–5965. <https://doi.org/10.1175/jcli-d-18-0681.1>
- Wu, X., Okumura, Y. M., & DiNezio, P. N. (2021). Predictability of El Niño duration based on the onset timing. *Journal of Climate*, 34(4), 1351–1366. <https://doi.org/10.1175/jcli-d-19-0963.1>
- Xie, P., & Arkin, P. A. (1997). Global precipitation: A 17-year monthly analysis based on gauge observations, satellite estimates, and numerical model outputs. *Bulletin of the American Meteorological Society*, 78, 2539–2558. [https://doi.org/10.1175/1520-0477\(1997\)078<2539:gpayma>2.0.co;2](https://doi.org/10.1175/1520-0477(1997)078<2539:gpayma>2.0.co;2)
- Yeh, S.-W., Kug, J.-S., Dewitte, B., Kwon, M.-H., Kirtman, B. P., & Jin, F.-F. (2009). El Niño in a changing climate. *Nature*, 461, 511–514. <https://doi.org/10.1038/nature08316>
- Yukimoto, S., Adachi, Y., Hosaka, M., Sakami, T., Yoshimura, H., Hirabara, M., et al. (2012). A new global climate model of the meteorological research institute: MRI-CGCM3—Model description and basic performance. *Journal of the Meteorological Society of Japan*, 90, 23–64. <https://doi.org/10.2151/jmsj.2012-a02>
- Yun, K. S., Lee, J. Y., Timmermann, A., Stein, K., Stuecker, M. F., Fyfe, J. C., & Chung, E. S. (2021). Increasing ENSO–rainfall variability due to changes in future tropical temperature–rainfall relationship. *Communications Earth and Environment*, 2, 43. <https://doi.org/10.1038/s43247-021-00108-8>
- Zhou, T. J., Wu, B., Wen, X. Y., Li, L. J., & Wang, B. (2008). A fast version of LASG/IAP climate system model and its 1000-year control integration. *Advances in Atmospheric Sciences*, 25, 655–672. <https://doi.org/10.1007/s00376-008-0655-7>